

A NEW MEASUREMENT OF THE ${}^7\text{Li}(\text{d},\text{p}){}^8\text{Li}$ CROSS SECTION AND CONSEQUENCES FOR ${}^7\text{Be}(\text{p},\gamma){}^8\text{B}$.

L. Weissman¹, C. Broude¹, G. Goldring¹, R. Hadar¹,
M. Hass¹, F. Schwamm^{1,2} and M. Shaanan³

1.- Department of Particle Physics, The Weizmann Institute of Science
Rehovot, ISRAEL.

2.- Ruprecht-Karls Universität, Heidelberg, GERMANY

3.- Institute of Solid-State Physics, The Technion, Haifa, ISRAEL.

(February 28, 2018)

Abstract

A novel scheme for measuring the cross section of the ${}^7\text{Be}(\text{p},\gamma){}^8\text{B}$ reaction, the major source of high energy neutrinos from the sun, is presented. The scheme involves a strictly uniform particle beam and overcomes some of the recognized experimental uncertainties of previous measurements. A new measurement of $\sigma[{}^7\text{Li}(\text{d},\text{p}){}^8\text{Li}]$ has been carried out using this setup, and the present value of $\sigma[{}^7\text{Li}(\text{d},\text{p}){}^8\text{Li}] = 155(8)$ mbarn at the top of the $E_d(\text{lab.}) = 776$ keV resonance is compared to previous measurements. A new issue regarding both the (d,p) and (p, γ) reactions has been examined: reaction-product nuclei which are backscattered out of the target. Measurements and simulations carried out in the course of this investigation are presented and discussed in the context of possible effects on the measured cross sections of these reactions.

PACS Numbers: 95.30.Cq; 96.60.Kx; 25.45.Hi

I. INTRODUCTION

The cross section of the reaction ${}^7\text{Be}(p,\gamma){}^8\text{B}$ has recently become the subject of renewed intense scrutiny [1] owing to the pre-eminence of the ${}^8\text{B}$ reaction products as the main source of high energy neutrinos in the interior of the sun and, hence, the possible implications for the so-called ‘‘solar neutrino problem’’. A number of new precision measurements of this cross section in various stages of preparation have been reported lately. We have set up an experiment for such a measurement at the Weizmann Institute, focusing on one of the major sources of uncertainty in previous experiments: the homogeneity of the areal density of the target material.

In general, when a nonuniform particle beam impinges on a nonuniform target, the reaction yield is given by:

$$Y = \sigma \int \frac{dn_b}{dS} \frac{dn_t}{dS} dS \quad (1)$$

where n_b, n_t are the respective total numbers of beam and target particles and $\frac{dn_b}{dS}, \frac{dn_t}{dS}$ are areal densities.

Only when the target is known to be uniform and the beam is smaller than the target can eq.(1) be simplified to:

$$Y = \sigma \frac{dn_t}{dS} \int \frac{dn_b}{dS} dS = \sigma \frac{dn_t}{dS} n_b \quad (2)$$

In such a case, the evaluation of the cross section is independent of the areal distribution of the particle beam. On the other hand, in other cases - e.g. for radiochemically produced ${}^7\text{Be}$ targets [2] - the target cannot be assumed to be strictly uniform and the full relation (1) has to be used in the evaluation. The inherent uncertainties in the distributions $\frac{dn_b}{dS}$ and $\frac{dn_t}{dS}$ may thus lead to considerable uncertainties in the value of the integral and hence in the deduced cross section. We have addressed this problem by inverting the arrangement: we use a homogeneous beam - produced by raster scanning - impinging on a target smaller than the beam. The relation (1) then reduces to:

$$Y = \sigma \frac{dn_b}{dS} n_t \quad (3)$$

independent of the potentially problematic determination of the target areal distribution.

As a first step we measured the cross section of the reaction ${}^7\text{Li}(d,p){}^8\text{Li}$ at the top of the resonance at $E_d(\text{lab.})=776$ keV. The mirror nuclei ${}^8\text{Li}$ and ${}^8\text{B}$ have very similar mean lives and similar β decays (β^- and β^+ , respectively) to ${}^8\text{Be} \rightarrow 2\alpha$. The main differences are (i) the much easier preparation of a ${}^7\text{Li}$ target and (ii) the much higher yield from ${}^7\text{Li}(d,p)$. The reaction ${}^7\text{Li}(d,p){}^8\text{Li}$ can therefore provide a convenient check of the equipment and the

method. Beyond that, this reaction is of significance in its own right and as a stepping stone and calibration in some ${}^7\text{Be}(p,\gamma){}^8\text{B}$ experiments [1-4].

In the course of the present investigation we have examined a new issue: reaction-product nuclei being backscattered from the target backing, leaving the target assembly and reducing the number of detected α particles. We present below experimental results which probe this issue and compare them to computer simulations. The influence of this effect on past and future measurements is discussed.

II. EXPERIMENT AND PROCEDURE

The general scheme of the experiment is shown in Fig. 1a. A d_2 beam out of the Weizmann Institute 3 MV Van de Graaff accelerator is raster scanned over a rectangle of 7 mm \times 6 mm. The purpose of the scan is to obtain a beam of uniform areal density. The d_2 beam (as well as the p beam, see below) is collimated by a 3 mm diameter hole and impinges on a circular target of LiF of 2 mm diameter, evaporated on Al and Pt foils (see discussion below); the target spot is aligned with a set of variable collimators downstream of the target. The target is mounted on an arm which is periodically moved out of the beam and in front of a 40 micron surface barrier detector registering the delayed α 's following the β decay of ${}^8\text{Li}$. The detector was surrounded by a shroud to prevent scattered beam particles from reaching the detector. The time sequence of the whole cycle is: a.- 1.5 s beam-on-target; b.- 100 ms rotation; c.- 1.5 s of target in the counting position; d.- 100 ms rotation. In the counting position a gate signal from the control unit opens the ADC for α counting and the gated scaler for Faraday-cup beam monitoring. This sequence results in an efficiency factor for the α count (see below) of $\eta(\text{cycle}) = 0.400(1)$ (Fig. 1b). A liquid nitrogen cold cryofinger is placed close to the target area to protect the target surface from contamination. The vacuum in the chamber was $8 \cdot 10^{-7}$ torr.

The beam density $\frac{dn_b}{dS}$ was measured by collimating the beam by a series of holes of known areas downstream from the target position, integrating the collimated beam in an electron-suppressed Faraday cup and counting the digitized counts in a gated scaler. The current digitizer and the scaler were checked during the experiment with a calibrated current source. The beam homogeneity was virtually insured by the nature of the raster operation: a low frequency triangular y scan and a high frequency triangular x scan, in small, digitally controlled steps in clock-fixed time intervals. The beam homogeneity was checked in two direct ways: 1.- by measuring the areal density of x-rays from a tin foil induced by the scanned proton beam in a phosphor image plate (Fig. 2a, see Ref. 5), 2) by repeating the measurement with different downstream collimators of know apertures. For

a homogeneous beam the Faraday-cup counts of the integrated beam, normalized to the α yield, should be proportional to the area of the hole (Fig. 2b). The collimator hole areas were measured to an accuracy better than 1% by a microscope and by having an alpha source in front of the collimator-detector assembly. The number n_t of ${}^7\text{Li}$ nuclei in the 2 mm target was determined in a similar measurement using the reaction ${}^7\text{Li}(p,n){}^7\text{Be}$ with a proton beam of 1.985 MeV (Refs. 6 and 7). The same downstream beam collimator of 1.5 mm diameter was used in both measurements. The number of ${}^7\text{Be}$'s produced was measured by registering γ 's from the beta decay ${}^7\text{Be}\rightarrow{}^7\text{Li}^*$ (478 keV) in a Ge detector at the low-background counting laboratory of the NRC-Soreq Center. We have also taken care to adjust the plate-voltage to ensure the same area for both the p and d_2 beams, respectively.

For the ratio of the two yields we get from (1):

$$\frac{Y({}^8\text{Li})}{Y({}^7\text{Be})} = \frac{\sigma({}^8\text{Li}) n_d}{\sigma({}^7\text{Be}) n_p} \quad (4)$$

where n_d, n_p refer, respectively, to the total number of deuterons and protons registered. The number of ${}^8\text{Li}$ products, $Y({}^8\text{Li})$, is evaluated from the measured α counts:

$$n_\alpha = Y({}^8\text{Li})\eta(\alpha)$$

and $Y({}^7\text{Be})$ is evaluated from the measured γ counts of the radioactive decay of ${}^7\text{Be}$:

$$n_\gamma = Y({}^7\text{Be})\eta(\gamma)$$

The efficiency factors $\eta(\alpha)$ and $\eta(\gamma)$ above are each products of individual and independent efficiency factors detailed below. Inserting the expressions for n_α and n_γ into (4) we obtain the ${}^7\text{Li}(d,p){}^8\text{Li}$ cross section in terms of the ${}^7\text{Li}(p,n){}^7\text{Be}$ cross section and measured quantities:

$$\sigma_{(d,p)} = \sigma_{(p,n)} \frac{n_\gamma n_p \eta(\gamma)}{n_\alpha n_d \eta(\alpha)} \quad (5)$$

A. The α -particle counting efficiency - $\eta(\alpha)$

1. *The solid angle.*

The detector solid angle was defined by a collimator of diameter $d=8.14(3)$ mm which was placed at a distance $\ell = 81.92(10)$ mm from the target in the counting position. The solid angle is given by: $\Omega = \frac{1}{16} \frac{d^2}{\ell^2} = 6.16(6) 10^{-4}$ of 4π .

2. *The time-sequence efficiency - $\eta(\text{cycle})$*

This factor relates to the time fraction of the α counting out of the entire irradiation-counting cycle. From the description above and following Refs. 2,3, this factor is

calculated to be: $\eta(\text{cycle}) = 0.400(1)$. The time intervals of the rotation cycle were measured by counting a time-reference signal in the scaler gated by the cycle time windows (Fig. 1b).

3. *The spectral efficiency.*

The α spectrum in Fig. 3. was integrated from the point marked in the figure all the way to the top energy. The cutoff entailed a loss of low energy α 's on one hand and on the other - the inclusion of the high energy tail of the noise spectrum. These two quantities were estimated by rough extrapolations to be considerably less than 1% and approximately equal and hence the integration error appears to be negligible. The low energy tail of the α spectrum was also evaluated directly from the measured α spectrum in Ref. 8 folded with the energy loss of the α 's in the target, yielding a lost fraction of 0.2%.

B. The γ counting efficiency - $\eta(\gamma)$

1. *The γ branch.*

The γ branch of the decay of ${}^7\text{Be}$ to the first excited state of ${}^7\text{Li}$ at 478 keV is 0.1052(6) [9].

2. *Absolute calibration of the ${}^7\text{Be}$ activity.*

The activity of the ${}^7\text{Be}$ 478 keV γ -ray source produced in the (p,n) reaction on the various targets was determined by comparison with calibrated ${}^{22}\text{Na}$, ${}^{137}\text{Cs}$ and ${}^{133}\text{Ba}$ γ sources at a fixed distance from a Ge detector, shielded for low-background, at the γ -counting laboratory of the NRC-Soreq Center. ¹ The absolute intensities of the γ sources used are known to within 2.5 - 3% each. The number of 478 keV γ rays (and hence the number of ${}^7\text{Li}$ nuclei in the target) is thus determined to an accuracy of 3%.

3. *The β decay of ${}^7\text{Be}$.* The LiF targets were bombarded by protons for several hours and γ 's were counted for about a day a short time later. The number of ${}^7\text{Be}$'s was inferred from the number of γ counts through the relation:

$$n_{\gamma} = n_{\text{Be}} \frac{t_1}{\tau} \exp(-t/\tau) \eta(1) \eta(2)$$

¹ The laboratory is designated as an International Reference Center for Radioactivity (IRC) by the World Health Organization.

where t_1 is the γ counting time, t is the time from the middle of the p run to the middle of the counting time, τ is the ${}^7\text{Be}$ mean life: $\tau = 76.88$ d [9] and $\eta(1)$ and $\eta(2)$ are the efficiency factors referred to above.

C. Other quantities in eq. (5)

1. Current integration.

The quantity $\frac{n_d}{n_p}$ is the ratio of scaler counts from a current integrator monitoring the current in the Faraday cup for the d_2 and p beams, respectively, using the same collimator hole. The construction of the Faraday cup, including the suppressor, ensures a reliable monitoring of the current. A calibrated current source was used to check the accuracy of the current integrator. In any case, as only the *ratio* of the counts enters the cross-section determination, any possible error from this source cancels out in first order.

2. Counting statistics - $\frac{n_\gamma}{n_\alpha}$.

The statistical errors of the α and γ counts were typically 0.5% and 0.7%, respectively for all the targets used. There is in addition a 1% systematic error in the γ counting due to uncertainties in the background subtraction procedure.

3. The ${}^7\text{Li}(p,n){}^7\text{Be}$ cross section.

The cross section for this reaction exhibits a flat and constant region around the beam energy of $E_p = 1.985$ MeV employed in this experiment. The cross section at this energy was taken from Refs. 6,7, which are in very good agreement with each other. Each of these references quotes, separately, an absolute error of 5%. We therefore adopt the value of $\sigma[{}^7\text{Li}(p,n){}^7\text{Be}] = 269(9)$ mb at $E_p = 1.985$ MeV.

Table I presents a summary of the experimental errors discussed above.

Another source of error which was considered is the production of ${}^7\text{Be}$ by ${}^6\text{Li}(d,n){}^7\text{Be}$, adding on to the ${}^7\text{Be}$ produced by ${}^7\text{Li}(p,n){}^7\text{Be}$. The added fraction was evaluated from the known cross-sections [10] and the fraction of ${}^6\text{Li}$ in the target to be less than 0.2% and therefore insignificant.

A larger correction to the extracted cross section can arise from the effect of ${}^8\text{Li}$ lost from the target due to backscattering. This issue is discussed in III.

D. d_2 and p energy calibration.

A d_2 beam at the 776 keV resonance corresponds to an accelerator voltage of 1.552 MV. The voltage was calibrated using the known thresholds of the $^{13}\text{C}(p, \gamma = 9.17 \text{ MeV})^{14}\text{N}$ reaction at 1.746 MeV and the $^7\text{Li}(p,n)^7\text{Be}$ reaction at 1.88 MeV which are close to the d_2 and p beam voltages.

III. BACKSCATTERING OF REACTION-PRODUCT NUCLEI

In the course of this experiment it became apparent that under some conditions the backscattering of recoil nuclei out of the target can be significant and can affect the cross section measurements. In order to obtain a quantitative estimate of these effects, the propagation of the reaction products of the $^7\text{Li}(d,p)^8\text{Li}$ and $^7\text{Be}(p,\gamma)^8\text{B}$ reactions was simulated with the aid of the TRIM [11] code. We have also determined these effects experimentally for the (d,p) reaction.

A. Backscattering for $^7\text{Li}(d,p)^8\text{Li}$ and $^7\text{Li}(p,n)^7\text{Be}$

For the $^7\text{Li}(d,p)^8\text{Li}$ reaction one has to take into account the broad angular distribution of the protons [12] (and the ^8Li recoils) and also to evaluate the loss of the backscattered ^7Be 's from $^7\text{Li}(p,n)^7\text{Be}$ reaction, used as a standard (see section II). One can then infer the total effect of backscattering loss on the cross-section measurement.

Calculations were carried out for LiF targets on Pt, Ni and Al backings at 776 keV deuteron energy. The results presented here are an average of simulations of reactions occurring at three positions in the LiF target. At a given depth in the LiF target the energy and angular distribution of ^8Li ions were evaluated and used to obtain the angle and energy distributions of the backscattered ^8Li ions from TRIM. The backscattered nuclei were then traced in the direction opposite to the beam to obtain the number of ions leaving the target.

A similar procedure was carried out for the backscattered ^7Be from the $^7\text{Li}(p,n)^7\text{Be}$ reaction for the proton beam energy of 1.99 MeV. The angle and energy distributions of the neutrons (and the ^7Be recoils) were taken from Ref 13. The results of the TRIM simulation are shown in Table II. As we see from the table, the effect of backscattered particles can give rise to a sizeable correction for high Z substrates.

B. backscattering for ${}^7\text{Be}(\text{p},\gamma){}^8\text{B}$

Similar backscattering effects also exist for the ${}^7\text{Be}(\text{p},\gamma){}^8\text{B}$ reaction. In this case, the kinematics of the reaction is much simplified as the ${}^8\text{B}$ nuclei from the proton-capture reaction all proceed in the proton-beam direction with the same center-of-mass momentum. As an example we have performed calculations which duplicate the conditions of Ref. 2. In that experiment the target was electroplated on polished Pt disks and contained 7 μg of solid material with 11% of ${}^7\text{BeO}$ [14]. For low proton energy, the number of backscattered particles depends very strongly on the (unknown) target composition. Two hypothetical trial cases are shown in Fig. 4. The first is for ${}^7\text{BeO}$ dissolved in pure iron; the second case is for a hypothetical composition of equal number of CuO , Cu_2N_3 and C molecules. The latter composition has been chosen following the statement in Ref. 14 that the solid materials remaining after the plating and flaming procedure are most likely to be traces of light metal oxides, nitrates and carbon. It is obvious from Fig. 4 that heavy atoms in the target and target backing should be avoided as much as possible in precision measurements of the ${}^7\text{B}(\text{p},\gamma){}^8\text{B}$ cross section.

C. Backscattering measurements for the ${}^7\text{Li}(\text{d},\text{p}){}^8\text{Li}$ reaction.

We have used several LiF targets with Al and Pt backing materials in order to probe experimentally the backscattering issue. The results of the cross section measurements for five targets, together with the backscattering fraction as calculated by TRIM, are presented in Table III. The error of each measurement is about 5% (Table I). The experiments yield a 9.1(2.2) % difference between the 400 \AA LiF on Pt and the LiF on Al targets. The relative error for the two types of targets is smaller than the individual errors since it does not include the common uncertainties of the ${}^7\text{Li}(\text{p},\text{n}){}^7\text{Be}$ cross section and the γ -detector efficiency. The TRIM simulations are in good agreement with the experimental results.

IV. RESULTS AND CONCLUSION.

As the final result of the ${}^7\text{Li}(\text{d},\text{p}){}^8\text{Li}$ cross section we have adopted an average of the two aluminum-backed targets, believed to be free from the backscattering loss. We get: $\sigma[{}^7\text{Li}(\text{d},\text{p}){}^8\text{Li}] = 155(8)$ mbarn.

A recommended value for this cross section is given in Ref. 1 : $\sigma = 147(11)$ mbarn. This value is based on four measurements, two of which should be corrected for backscattering

loss. Based on the available target details as presented in the respective publications, we estimate the corrected value to be in the range 150 - 152 mbarn, very close to our value.

Previous measurements of the $\sigma(^7\text{Be}(p,\gamma)^8\text{B})$ cross section are also susceptible to backscattering losses. In particular, the results of Ref. 2 should be corrected for both the $^7\text{Be}(p,\gamma)^8\text{B}$ and the $^7\text{Li}(d,p)^8\text{Li}$ reactions. The $^7\text{Be}(p,\gamma)^8\text{B}$ reaction was measured at various energies and, as can be seen from Fig. 4, the backscattering correction diminishes at low energies. The $^7\text{Li}(d,p)^8\text{Li}$ reaction at the resonance energy was then used by the authors to obtain the number of ^7Li , and hence ^7Be , atoms in the same platinum-backed target. Since the correction due to this is a *constant* which is of the opposite sign and larger than the ^8B corrections (Table II and Fig. 4), the overall effect is to reduce the derived S factor, especially at lower energies.

We would like to express our sincere thanks to Ygal Shahar for his expert help in operating the Van de Graaff accelerator and in constructing the beam line. We wish to thank Meir Birk and Moshe Sidi for designing and constructing the raster scanner, and Leo Sapir and Boris Levine for the target preparation. We acknowledge with thanks the expert help of Ovadya Even of the Soreq Center in the γ -efficiency calibration. We are grateful to Prof. Claus Rolfs for extensive and enlightening discussions.

REFERENCES

- [1] E.G. Adelberger et al., to be published in Rev. Mod. Phys.
- [2] B.W. Filippone, A.J. Elwyn, C.N. Davids and D.D. Koetke, Phys. Rev. **C28**, 2222 (1983).
- [3] B.W. Filippone, A.J. Elwyn and W. Ray, Jr., Phys. Rev. **C25**, 2174 (1982).
- [4] F. Strieder, L. Gialanella, U. Greife, C. Rolfs, S. Schmidt, W.H. Schulte, H.P. Trautvetter, D. Zahamow, F. Terrasi, L. Campajolla, A.D'Onorfrio, V. Roca, M. Romano and M. Romoli, Z. Phys. **A 355**, 209 (1996).
- [5] L. Weissman, M. Hass and V. Popov, Nucl. Inst. Meth. **A400**, 409 (1997).
- [6] K.K. Sekhran, H. Laumer, B.D. Kern and F. Gabbard, Nucl. Inst. Meth. **133**, 253 (1976).
- [7] R.L. Macklin and J.H. Gibbons, Phys. Rev. **114**, 571 (1959).
- [8] E.K. Warburton, Phys. Rev. **C33**, 303 (1986).
- [9] Table of Isotopes, 8th edition, J. Wiley and Sons, New York (1996).
- [10] C. R. McClenahan and R. E. Segel, Phys. Rev. **C11**, 370(1986)
- [11] H.H. Andersen and J.F. Ziegler, *The Stopping and Ranges of Ions in Matter* (Pergamon, New York, 1977, Vol. 3.)
- [12] J.P.F. Sellschop, Phys. Rev. **119**, 251 (1960).
- [13] H. Liskien and A. Paulsen, Atomic and Nuclear Data Sheets, **15**, 57 (1984).
- [14] B. W. Filippone and M. Wahlgren, NIM, **A243** (1986) 41-44.

FIGURES

FIG. 1. 1a - Schematic view of beam line; the beam scanner and measuring chamber are indicated. 1b - The time sequence of the stepping motor rotation, irradiation and data acquisition.

FIG. 2. Scanned-beam uniformity measurements. a - A one-dimensional intensity cut of the x-ray yield from the molecular plate [5]. b - The d_2 count in the Faraday cup, normalized to the α yield, as a function of collimator area.

FIG. 3. A typical α spectrum.

FIG. 4. Results of the TRIM simulations for the ^8B backscattering loss for the conditions of Ref. 2, assuming two different target compositions: circles - ^7BeO dissolved in pure iron; squares - ^7BeO dissolved in equal amounts of CuO , Cu_2N_3 and C molecules.

TABLES

TABLE I. Compilation of experimental errors.

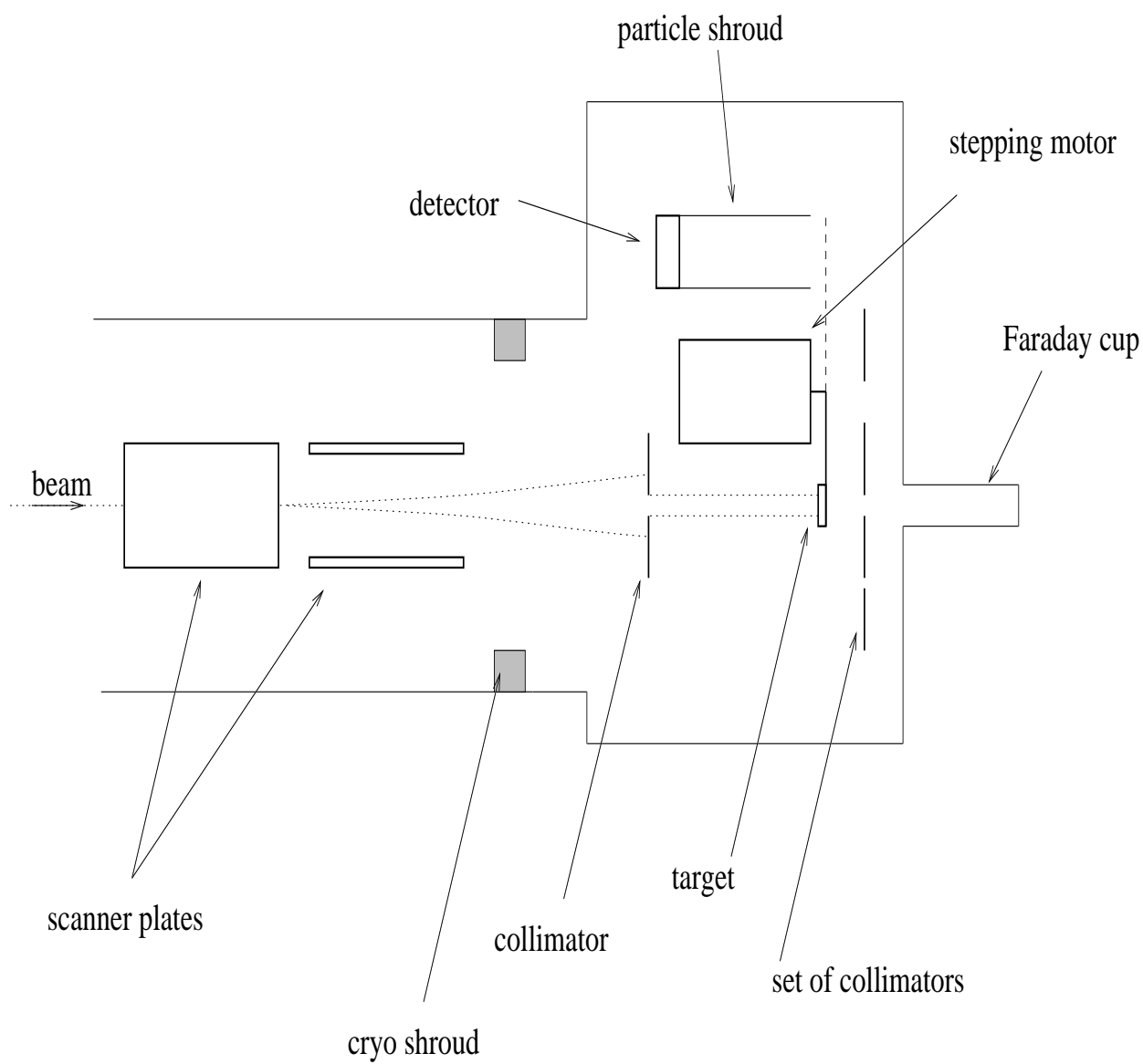
The source of the experimental error	Error (%)
Uncertainty in $\sigma_{(p,n)}$	3.5
Absolute efficiency of γ counting	3
Systematic error in γ counting	1
Statistics of gamma counting	0.7
Statistics of alpha counting	0.5
Solid angle of α detector	0.5
γ branch for ${}^7\text{Be}$ decay	0.6
Timing of the rotating cycle	0.3
Total	≈ 5

TABLE II. The results of TRIM simulation for the number of backscattered particles in ${}^7\text{Li}(d,p){}^8\text{Li}$ and ${}^7\text{Li}(p,n){}^7\text{Be}$ reactions for three different backing materials

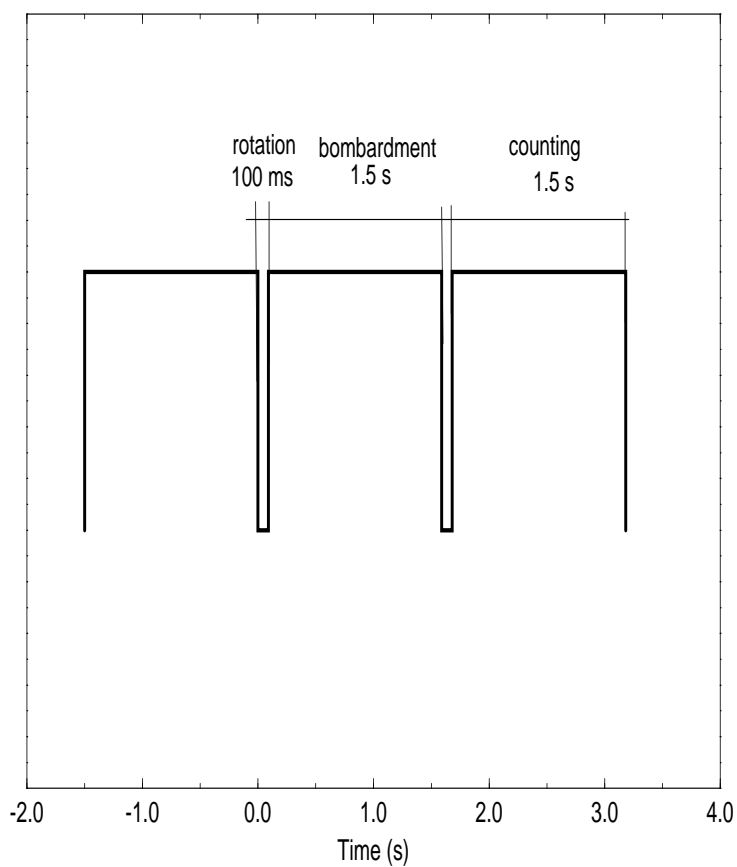
Backing material	Thickness of LiF (\AA)	Lost fraction of ${}^8\text{Li}$ (%)	Lost fraction of ${}^7\text{Be}$ (%)	Correction to cross-section (%)
Pt	1000	12.9(1.5)	5.1(1.0)	7.4(1.8)
Pt	400	15.6(1.5)	5.8(1.0)	9.8(1.8)
Ni	1000	2.4(1)	1.3(0.7)	1.1(0.9)
Al	1000	0.3(0.5)	0.07(0.1)	0.25(0.6)

TABLE III. The results of cross section measurements for the different targets.

Backing material	Thickness of LiF \AA	$\sigma_{d,p}/\sigma_{p,n}$	$\sigma_{d,p}$ (mbarn) (mbarn)	$\sigma_{d,p}$ (mbarn) corrected by TRIM
Al	1100	0.57(2)	154(8)	154(8)
Al	1100	0.57(2)	156(8)	156(8)
Pt	1200	0.54(2)	146(8)	156(10)
Pt	400	0.53(2)	143(8)	157(10)
Pt	400	0.52(2)	140(8)	154(10)
Adopted value			155(8)	

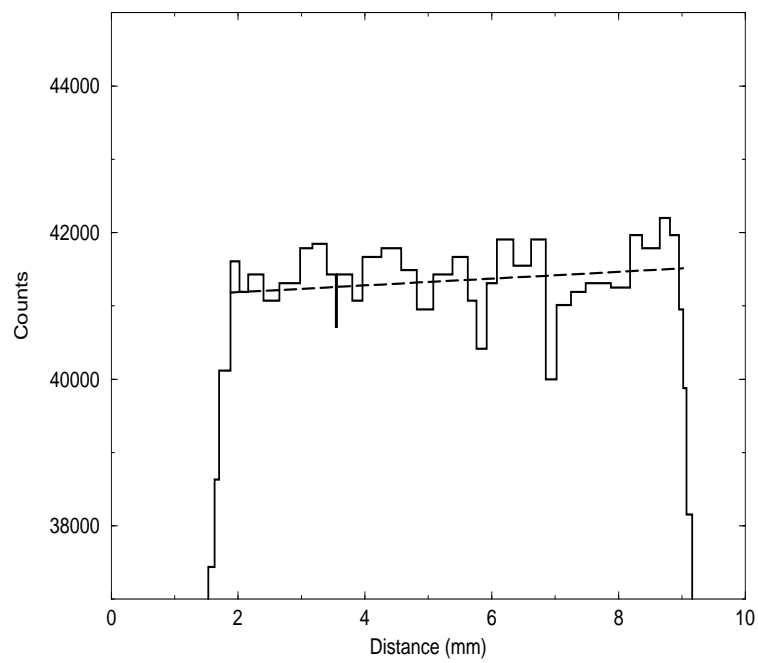


a)



b)

a)



b)

